JACOBS PUBLISHERS

OPEN ACCESS

Jacobs Journal of Cell and Molecular Biology

Review Article

Mitochondria and Vascular Sensitivity during Long-term Morphine Exposure

Hui Zhao*[1], Huilin Mou[1], Xiaojian Li[1], Han-Wei Huang[2]

[1]*Department of Integrative Medicine and Neurobiology, National Key lab of Medical Neurobiology, Institute of Brain Research Sciences, Shanghai Medical College, Fudan University*

[2]*Department of Orthopaedics, Shanghai 5th Hospital, Fudan University*

**Corresponding author:* *Dr. Hui Zhao, Department of Integrative Medicine and Neurobiology, Shanghai Medical College, Fudan University, China, 138# Yixueyuan Rd. Box 291, Shanghai, 200032, P.R.China, Tel: 86-21-54237611; Fax: 86-21-54237023; Email: zhaohui07054@fudan.edu.cn*

Received: 10-10-2014

Accepted: 12-19-2014

Published: 03-09-2015

Abstract

Microenvironment adaptation was proposed to be interoceptive cues for conditioned morphine dependence and tolerance. In the present study, we revealed in prefrontal cortex, that there was apparent mitochondrial and vascular oxidant production following long-term morphine treatment and subsequent naloxone precipitation. Comparably, naloxone precipitation equipped a higher capacity in modulation of VEGF-VEGFR2 signaling and close connection of VEGFR2 and AC5. Moreover, it was observed that alternative GR promoter usage was related with vascular and mitochondrial sensitivity and individual CREB activation, in which GR-1C and reflected GRalpha were involved in chronic morphine treatment, while GR-1B and reflected GRp were biased initiated by naloxone precipitation. Of most interest, by using mice subjected to predator stimulator stress (PSS), it was demonstrated that oxidant production and expressions of GRp and GRalpha could be cross-sensitized by morphine. Intriguingly, mice with PSS exhibited deteriorated behaviors in morphine withdrawal and place conditioning, but not antinociceptive tolerance, the responses were more related with GRp than GRalpha. Therefore, our results unveiled a pivotal role of mitochondrial and vascular environment in the maintaining and potentiation of neuro-adaptive morphine activities, increasing vulnerability of GRp to vascular remodeling was thought to be critical for morphine withdrawal.

Introduction

Morphine (Mor) has been used for centuries to alleviate pain, however, its use is limited by a number of adverse consequences, such as constipation, respiratory suppression, and the potential development of dependence and addiction after extended periods of administration [1-2]. It has been greatly strengthened that physiological actions of morphine are principally mediated through μ-opioid receptor (MOR) [3-5], for example, the initially decreases in cAMP levels by MOR activation could be restored during continued exposure to morphine (tolerance), and even are increased further (superactivation) upon opiate receptor blockade or opiate withdrawal [6-7], therefore, cAMP pathway was thought to be critical adaptive changes in models of addiction [8-12].

Human genetic study has revealed an association between microenvironment and risk of opioid tolerance and dependence [13-14]. Interoceptive cues provided by the up-regulation of proinflammatory cytokines might be sufficient stimuli to a conditioned morphine withdrawal severity [15-17]. Previously, it was characterized that mitochondrial and vas-

cular oxidant production were superior potency for proinflammatory responses (lipopolysaccharide, TNF-α, IL-1, and IL-6) [18-22], especially, vascular endothelial growth factor receptor (VEGFR) could be distinctively modulated by mitochondrial biogenesis and vascular XO activity, the signaling cascades were thought to implicate in ER related subcellular communication and required for morphine mediated AC5 superactivation [23-24]. We thus proposed a teleological argument that mitochondrial and vascular sensitivity might be adapted and contribute to activation of cAMP signaling during long-term morphine exposure.

As characterized, stressful experience initiates a neuroendocrine response, the glucocorticoid receptor (GR) activation is a metaplastic signal that allows somatodendritic opioid release, and a persistent retrograde suppression of synaptic transmission through presynaptic MOR [25-27], in return, chronic opioid use leads to structural reorganization of GR-dependent genes, and GR mRNA is more sensitive to episodes of morphine withdrawal [28-29]. Lately, several SNPs in the GR-gene have been tested for functionality, differential promoter usage including promoter1B, 1C, 1D, 1F and 1H were demonstrated to implicate in distinctive cellular events [30-32]. Therefore, in the present study, mice with chronic stress was established, by which determined to define functional phenotype of GR in mitochondrial and vascular adaption during morphine dependence and tolerance.

Materials and Methods

Morphine treatments

Mice were s.c. injected with escalating doses of morphine twice daily for 5 days. On day 6, mice were injected with 1 mg/kg naloxone 2h after 100 mg/kg morphine treatment. Mice were placed in transparent cylinder (50x30cm) for 30 min, the somatic signs of jumps, wet dog shakes, paw tremor, rear and grooming were monitored and quantified. Morris Water Maze was performed [33]. In the acquisition section, mice were placed in the water maze (122 cm diameter) with the platform (10 cm diameter) submerged in the SW quadrant. In the extinction section, mice were placed in the NE quadrant of the water maze without the platform for 60s. The amount of time mice spent in each quadrant searching for the platform was recorded. Additionally, hot-plate test was performed, the cutoff time was set at 10s, antinociceptive response is expressed as mean $\pm$ S.E.M. of percentage of the maximum possible effect (%MPE).

For treatments, mice were positioned in a Kopf stereotaxic apparatus with burr holes drilled into the skull, a 5μl Hamilton syringe fitted with a 33-gauge needle was lowered into prefrontal cortex for drug delivery. Adenovirus particles (5×109 plaque-forming units (PFU) dissolved in sterilized PBS was injected over 10s via the needle at a volume of 2μl. All experimental procedures were approved by Ethics Committee of Fudan University, efforts were made to minimize the numbers of animal used and their suffering.

ELISA

Prefrontal cortex was dissected and homogenized in ice-cold lysis buffer containing 137mM NaCl, 10mM Tris-HCl, pH8.0, 1mM EDTA, pH 8.0, 1% NP-40, 10% glycerol, 1mM phenylmethylsulphonyl fluoride, 10mg/ml aprotinin, 1mg/ml leupeptin, and 0.5mM sodium vanadate. The tissue homogenate solutions were centrifuged at 14,000 × g for 5 min at 4°C. The supernatants were collected and used for quantification of total protein. Level of VEGF was assessed using a commercially available assay kit from Promega. Color change was measured in an ELISA plate reader at 450 nm.

Recombinant adenovirus construction

Recombinant adenovirus expressing mouse GRs were constructed and inserted into the adenoviral shuttle vector pDE1sp1A (Microbix Biosystems, Inc. Canada). For knocking down endogenous XO, PGC-1α, small interfering RNA duplexes were designed on the basis of the respective sequences. Constructs were cloned into adenoviral shuttle vector pDE1sp1A (Microbix Biosystems, Inc. Canada). After homologous recombination with the backbone vector PJM17, plaques resulting from viral cytopathic effects were selected and expanded in 293 cells.

Cell culture

N2A cells stably expressing HA-MOR or VEGFR2/VEGFRY1175F were cultured with advanced DMEM (Invitrogen) supplemented with 5% fetal bovine serum (HyClone), and 0.2 mg/ml G418 (Geneticin, Invitrogen) in a 5% CO2 atmosphere at 37°C.

For primary neuron culture, dissociated neurons were prepared from mice prefrontal cortex (embryonic day 15) and plated onto 35-mm Petri dishes at a density of 1×106 cells. 10 days later, neurons were undergone drug treatment. For co-culture model, microvascular fragments (MVFs) were isolated, briefly, prefrontal cortex collected from euthanized mice were minced and digested in a collagenase solution [2mg/ml in PBS containing 0.1% bovine serum albumin (BSA)] for 8–10 min. MVFs were pelleted by centrifugation, washed and resuspended in PBS containing 0.1% BSA. Isolated MVF were suspended in pH-neutralized rat tail type I collagen (3mg/ml final concentration using DMEM) at approximately 15,000 MVF/ml for plating (0.25 ml/well) in 48-well culture plates.

Oxidant production

Prefrontal cortex was homogenized in 0.1 M phosphate buffer (pH 7.4) with a motor-driven Polytron glass homogenizer at 4°C. The resulting homogenate was filtered through four layers of medical gauze to remove connective tissue debris. Oxidant generation was determined within 30min of tissue harvest in fresh tissue homogenates using dichlorofluorescein (DCF) as a probe. The basal buffer consisted of 0.1M potassium phosphate at pH7.4. The induced buffer additionally included 1.7mM ADP, 0.1mM NADPH, and 0.1mM FeCl3. Both buffers included 5μM 2′,7′-dichlorofluoresceindiacetate (DCFH-DA), which was made fresh in 1.25 mM methanol and kept in a dark room at 0°C. For basal condition, following reagents were added: 2938μl 0.1M phosphate buffer, 50μl filtered tissue homogenate, and 12μl 1.25 mM DCFH-DA. Induced condition was replaced 90μl of buffer with 50μl FeCl3, 20μl ADP, and 20μl NADPH. Total reaction volume was 3.0ml. A blank consisting of the appropriate buffer and 5.0μM DCFH-DA without sample was used to correct for the auto-oxidation rate of DCFH-DA. The mixture was incubated in the dark for 15 min at 37°C. DCF formation was determined with a Hitachi F-2000 fluorescence spectrophotometer (Hitachi Instruments, Co., San Jose, CA) with a thermostated cell compartment at excitation wavelength 488nm and emission wavelength 525nm. The units were expressed as pmol DCF/mg protein.

XO/XDH activity assay

Measurement of XO and XDH activity in prefrontal cortex was based on the pterin-based assay. In brief, approximately 40mg of tissues was homogenized in 1ml assay buffer (50mM K-phosphate, 1mM ethylene-diaminetetraacetic acid, 0.5% dimethyl sulfoxide, and proteaseinhibitor cocktail, pH7.4). The supernatant (150μl) was co-incubated with 50μl pterin solution (final concentration of 50μM) or pterin with methylene blue solution (final concentration of 50μM) to assay XO or both XO and XDH activities. Before and after 120min incubation at 37°C, fluorometric assay was performed to calculate the production of isoxanthopterin. Protein concentration was measured by Pierce BCA Protein Assay Kit (Thermo Scientific Inc., Billerica, MA, USA).

In vitro Src kinase assay

Proteins were separated and immunoprecipitated by anti-c-Src antibody (1:200; Abcam). The resulting pellets were washed with acetone and incubated at 30°C with 5μg of SRC substrate peptide (KVEKIGEGTYGVVYK, corresponding to amino acids 6-20 of p34cdc2; Upstate Biotechnology, Lake Placid, New York) in kinase buffer containing 5μCi of [γ-32P]-adenosine triphosphate ([γ-32P]-ATP; PerkinElmer Life Sciences, Waltham, Massachusetts), 50mM Tris-HCl (pH7.5), 10mM MgCl2, 10mM MnCl2, 25μM ATPase, 1mM dithiothreitol, and 100μM Na3VO4. After 30min, the reaction was terminated by the addition of 10μl of 40% (w/v) TCA, and samples were spotted on P81 cellulose phosphate paper (Upstate Biotech). The paper was washed three times with 1% (w/v) phosphoric acid and once with acetone. Radioactivity retained on the P81 paper was quantified by liquid scintillation counting. Blank counts (without tissue lysate) were subtracted from each result, and radioactivity (cpm) was converted to picomoles per minute (pmol/min).

Immunofluorescent labeling and fluorescent in situ hybridization (FISH)

Mice were anesthetized with sodium pentobarbital (35mg/100g, i.p.) and transcardially exsanguinated with 0.1M PBS followed by perfusion of the fixation (4% paraformaldehyde in 0.1M PBS, pH7.4), each provided in a 7ml/min flow rate. Serial sets of 20μm coronal brain sections were collected on a freezing microstome (Leica, SM2000R). Frozen sections were subsequently incubated with anti-VEGFR2 (1:500, Abcam; Cambridge, CB) and Alexa Fluor488 conjugated antibody, anti-MOR (1:500, Abcam; Cambridge, CB) and Alexa Fluor594 conjugated antibodies. Data derived from each group were analyzed by Leika Q500IW image analysis system.

Riboprobes were prepared from an open reading frame of GR subcloned into a pBluescriptIISK vector. Digoxigenin (DIG)-labeled probes were synthesized by T7 RNA polymerase with the DIG-RNA labeling mix (Roche Diagnostics) using linearized plasmid as template. In situ hybridization was performed with sense and antisense riboprobes overnight at 55°C. After hybridization, probes were detected using Alexa Fluor488-conjugated anti-DIG antibody. Data derived from each group were analyzed by Leika Q500IW image analysis system. Hybridization density is reported as the average density of all individual animals ± SEM in each experimental group (n = 5). The mean density of all the microphotographs was analyzed with the aid of ImageJ analysis software.

Real-time PCR

Total RNA was isolated from tissue or cells, mRNA was extracted by UNIzol reagent and treated with RNase-free DNase I (Takara, Japan). Reverse transcription using random hexamers was performed with Omniscript reverse transcriptase (QIAGEN, Los Angeles, CA). Real-time PCR analysis was performed with the cDNA product from 50 ng RNA per well on an ABI Prism 7700 (Applied Biosystems, Foster City, CA). Each sample was analyzed in duplicate along with a corresponding sample with no reverse transcriptase was added (no reverse transcriptase control). PCR conditions for each primer pair were optimized in pilot experiments to amplify the desired product in the linear range of amplification, the general reaction conditions were as follows: 50°C for 2 min and 95°C for

10 min, followed by 40 cycles of 95°C for 15 sec and 60°C for 1 min. Gene expression was normalized to the expression of 18s rRNA and quantified with 2−ΔΔCt method, which computed the percentage change relative to control.

Immunoprecipitation and Western Blotting

Prefrontal cortex was homogenized and centrifuged, the supernatants were incubated with anti–AC5 (1:200; Santa Crutz Biotechnology; Santa Cruz, CA), anti-RSK2 antibodies (1:200; BD Transduction Laboratories, Lexington, KY) at 4°C overnight with slow rotation. 60µl of protein G–agarose beads (Invitrogen, Carlsbad, CA) were added and further incubated for 3h. Afterwards, the beads were washed and protein sample were eluted from with 1x SDS sample buffer.

For western Blot analysis, proteins were resolved in SDS-polyacrylamide gel, and transferred to polyvinylidene difluoride membrane (GE Healthcare, Piscataway, NY). The membrane was probed in the presence of anti-VEGFR2, VEGFR-Y1175 (1:1000, Abcam), anti-PGC-1α, anti-pCREB, anti-CREB (1:1000, Santa Crutz Biotechnology), respectively, then was incubated with secondary antibody conjugated with alkaline phosphatase, protein bands were detected by ECF substrate and scanned in the Storm 860 Imaging System, the band intensities were quantified and analyzed with the ImageQuant software (GE Healthcare).

Subcellular fractionation and HDAC Activity

For nuclear extracts, cells were washed twice in ice-cold PBS, resuspended in buffer A (10mM HEPES, 10mM NaCl, 3mM MgCl2, 1mM EGTA, 0.1% Triton X-100, pH7.5) supplemented with 50mM NaF, 1mM Na3VO4, 1mM DTT, 1mM PMSF, and 1µg/ml protease inhibitor cocktail and incubated on ice for 40 min. The nuclei were pelleted by centrifugation at 2400g for 10min at 4°C and resuspended in buffer B (25mM HEPES, 300mM NaCl, 5mM MgCl2, 1mM EGTA, 20% glycerol, pH7.4) supplemented with 50mM NaF, 1mM Na3VO4, 1mM DTT, 1mM PMSF, and 1µg/ml protease inhibitor cocktail. After incubation on ice for 60min, the lysates were centrifuged at 12,000g for 20 min at 4°C, the supernatants (nuclear extracts) were collected. HDAC activity was measured by a colorimetric HDAC activity assay (Biovision Research, Mountain View, California). Anti-acetyl histone H3-K14 (Millipore, Billerica, Massachusetts) was determined by Western Blot analysis.

BRET Assay

For the construction of VEGFR2-luciferase fusion protein, renilla luciferase coding sequence was amplified from pRL-null vector (Promega, Madison, WI) using sense and antisense primers harboring unique cloning sites (XbaI and ApaI). The PCR fragments were then inserted to yield constructs that were named VEGFR2-Rluc. Construction of plasmids for GFP2-AC5 fusion proteins were carried out by digesting AC5 coding sequences from their expression plasmids with HindIII and ApaI, and then inserting them in-frame into GFP2-C3 vector.
Cells were transiently transfected using Lipofectamine, 48 hours post-transfection, cells were detached with PBS/EDTA and resuspended in PBS containing 0.1% glucose (w/v) and 2µg/ml aprotinin, and then transferred to 96-well microplates (white Optiplate from BioSignal Packard Biosciences) at a density of 100,000 cells/well. Deep Blue C (coelenterazine; BioSignal Packard Biosciences) was added at a final concentration of 5µM, and readings were collected using a Fusion microplate analyzer (BioSignal Packard Biosciences) that allows the sequential integration of the signals detected in the 330-490 nm and 485-545 nm windows using filters with the appropriate band pass. The bioluminescence resonance energy transfer (BRET) signal is determined by calculating the ratio of the light emitted by the AC5-GFP (500-530 nm) over the light emitted by the VEGFR2-Rluc (370-450 nm). The values were corrected by subtracting background signal detected in vehicle-treated cells containing both Rluc or GFP2 proteins.

Glucocorticoid receptor genotyping

The CpG islands of 221 donors previously characterized for GR SNPs [33] were genotyped using standard PCR methods. Seven promoter fragments were amplified from genomic DNA using primers. PCR fragments were purified using the Jetquick PCR purification kit (Gemomed, DE). Purified products were sequenced using the BigDye 3.1 Terminator cycle sequencing reagent (Applied Biosystems, Nieuwerkerk, The Netherlands) on the ABI 3130 sequencer (Applied Biosystems) using the pMetLuc-sequencing primers. Sequences were analysed in Vector NTi (Invitrogen, Paisly, UK).

Statistical analysis-Data are presented as mean±S.E.M., either unpaired Student's t test (two-tailed) or a one-way analysis of variance was performed for statistical comparisons. Dunnett's multiple comparison was used to determine which conditions with significant different from the controls.

Results

Mitochondrial and vascular sensitivity during long-term morphine treatment

Chronic use of morphine is thought to induce microenvironment adaptations in brain, the changes were ultimately proposed to contribute to drug addiction phenotypes [1,2,34]. In the present study, oxidant production in the prefrontal cortex was firstly measured using DCF probe, in which the basal buffer condition measured predominantly nonmitochondrial sources of oxidant generation and maximum one could be stimulated by the induced buffer. As illustrated in Figure 1A,

oxidant production in the induced buffer was increased around 2.2-3.2 folds over control following long-term morphine treatment and subsequent naloxone precipitation, while oxidant production in the basal buffer could only be initiated by naloxone replacement. In accordance with this observation, XO and xanthine dehydogenase (XDH) activity were only sensitive to naloxone replacement, values increased around 3.0 folds over control (Figure 1B).

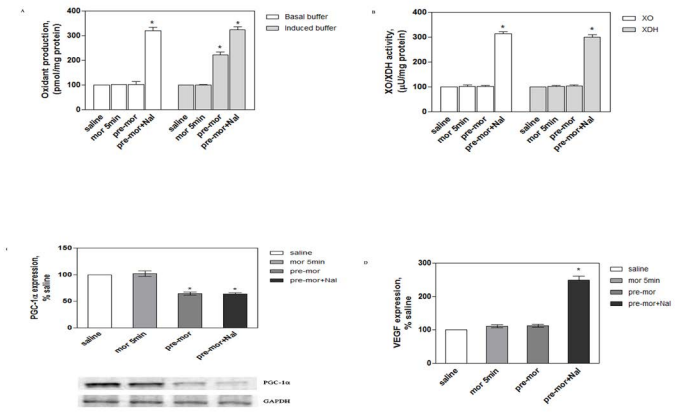

Figure 1. Mitochondrial and vascular sensitivity during long-term morphine treatment. Mice were undergone chronic morphine treatment and naloxone precipitation (n = 5 for each treatment), 4 days later, prefrontal cortex was extracted: A, oxidant production in induced or basal buffer were quantified by photocytometry assay, data was converted to pmol/mg protein; B, XO and XOH activity were quantified, data was converted to μU/mg protein; C, PGC-1α expression was detected by Western Blot analysis. D, VEGF production was measured by ELISA assay. Data are normalized and calculated as the percentage of control, each value is the mean±S.E.M. for 5 independent experiments. * P< 0.05 vs saline.

A number of physiological studies have established roles for peroxisome proliferators-activated receptor coactivator-1 α (PGC-1α) and VEGF signaling in mitochondrial biogenesis and vascular sensitivity respectively [35-37]. Consequently, by Western Blot analysis, it was illustrated that PGC-1α expression could be progressively down-regulated about 40% by long-term morphine treatment and subsequently naloxone precipitation (Figure 1C); by ELISA assay, VEGF production was dramatically enhanced following naloxone replacement (Figure 1D).

Connection of VEGFR-2 and AC5 during long-term morphine treatment

Given above observation, we assumed that VEGFR-2 signaling might correlate more with naloxone precipitation. By Western Blot analysis, it was illustrated that VEGFR2-Y1175 expression in prefrontal cortex dramatically rose to ~2.1 folds over control when challenged with naloxone replacement (Figure 2A). By immuno-fluorescent staining and immunoprecipitation, it was not surprising that in prefrontal cortex, VEGFR-2 and AC5 were co-localized, and their molecular connection was elevated around 2.4 folds over control after naloxone precipitation (Figure 2B, C).

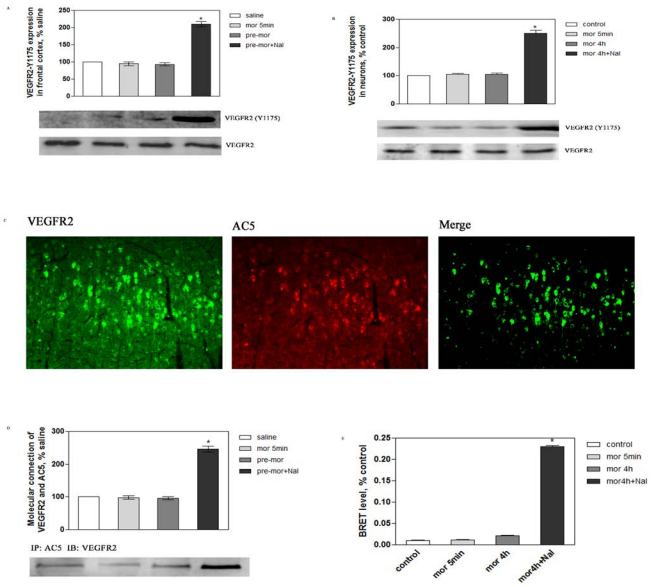

Figure 2. Connection of VEGFR-2 and AC5 during long-term morphine treatment. Mice were undergone chronic morphine treatment and naloxone precipitation (n = 5 for each treatment), 4 days later, prefrontal cortex was extracted. A, VEGFR-2 phosphorylation was determined by Western Blot analysis; B, connection of AC5 and VEGFR-2 was detected by immunoprecipitation, in which anti-AC5 was used as an immunoprecipitated antibody and anti-VEGFR-2 as an immunoblot antibody. C, cross section of prefrontal cortex were subsequently immuno-stained with anti-VEGFR2 and Alexa 488 antibody, anti-AC5 and Alexa 594 antibodies, each group were analyzed by Leika Q500IW image analysis system, Scale bar=50μm. D, cortical neurons were grown for 10 days, and co-cultured with vasculature in the presence of morphine for the indicated time, VEGFR2 phosphorylation was determined by Western blot analysis. E, N2A-MOR were transiently co-transfected with VEGFR-2-Rluc and GFP2-AC5 or GFP2 vector followed by chronic morphine treatment and subsequent naloxone precipitation, reading of the signals detected in the 370–450- and 500–530-nm windows, the BRET signal was determined by the ratio of the light emitted by the GFP2 or GFP2-AC5 (500–530 nm) over the light emitted by the VEGFR2-Rluc (370–450 nm). Data are normalized and calculated as percentage of control, each value represents mean±S.E.M of five independent experiments. *p<0.05 vs control or saline.

To ensure above crux event, in cortical neuron-vasculature co-culture, the sensitivity of VEGFR2-Y1175 could be enhanced by naloxone replacement (Figure 2D). Furthermore, BRET assay was performed, N2A-MOR were transiently co-transfected with VEGFR-2-Rluc and GFP2-AC5 or GFP2 vector, the expression levels of luciferase-tagged VEGFR-2 were controlled to be within 10% difference, the GFP and GFP-AC5 were blotted with anti-GFP antibody and quantified to be at about the same level

(data not shown). Figure 2E illustrated that nalxone replacement induced an increased interaction of VEGFR-2 and AC5, the plateau value of BRET ratio increase was 0.023±0.007.

Naloxone precipitated AC superactivation was not dependent on mitochondrial sensitive

Probably, the ability of VEGFR-2 and AC5 connection could tether AC5 inhibition, whose impairment was proposed to enable cAMP signaling amplification. In cortical neuron-vasculature co-culture, by Western Blot analysis, Figure 3A and B illustrated that AC5 expression was greatly elevated following 4h of morphine exposure and subsequent naloxone precipitation, intriguingly, the up-regulation could be interrupted when infected with PGC-1α siRNA. It was nearly matched with above observation, intracellular cAMP levels was firstly attenuated to around 50% control, and then increased to 104.6±13.4 and 343.8±32.5% control following 4h of morphine exposure and subsequent naloxone precipitation, PGC-1α knockdown resulted in partly inhibition in cAMP production (Figure 3C).

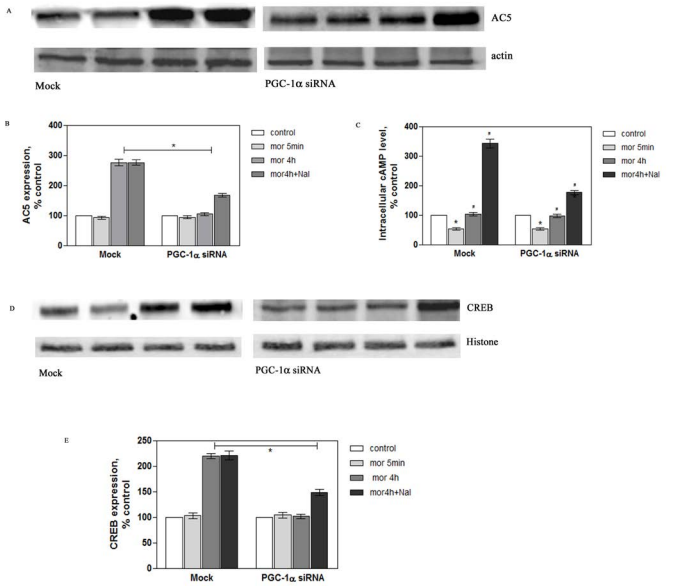

Figure 3. Naloxone precipitated AC superactivation was not dependent on mitochondrial sensitive. Cortical neurons were grown for 10 days, and co-cultured with vasculature in the presence of PGC-1α siRNA followed by chronic morphine treatment and subsequent naloxone precipitation. A and B, AC5 expression was determined by Western blot analysis; C, amount of intracellular cAMP production in the presence of 10μM forskolin was measured by AlphaScreen cAMP detection kit; D and E, CREB expression was detected by Western Blot analysis. Data are normalized and calculated as percentage of control, each value represents mean±S.E.M of five independent experiments. *p<0.05 vs control.

The transcription factor cAMP response element-binding protein (CREB) is likely related to a few signs of opiate withdrawal [38-46]. By Western Blot analysis, CREB expression was greatly increased following chronic morphine treatment and subsequent naloxone replacement. As anticipated, the up-regulation mediated by morphine was mostly dependent on PGC-1α (Fig3D, E).

Alternative expression of GR promoters during morphine treatment

The sequence variability within alternative GR promoter was investigated. By real-time PCR, it was demonstrated in Figure 4A that, promoter-1C could be initiated both by chronic morphine treatment and subsequent naloxone precipitation, and promoter-1B could only be up-regulated by naloxone precipitation. Coincidently, GRα mRNA expression displayed similar change pattern with that of promoter-1C, and GRp with promoter-1B. In neuron-vasculature co-culture, it was further illustrated that GRp expression could be up-regulated by naloxone precipitation, the effect was disrupted by VEGFR2 knockdown (Figure 4B). Comparably, chronic morphine initiated expressions of GR α and GRp could be inhibited by transfection of PGC-1 α siRNA (Figure 4C).

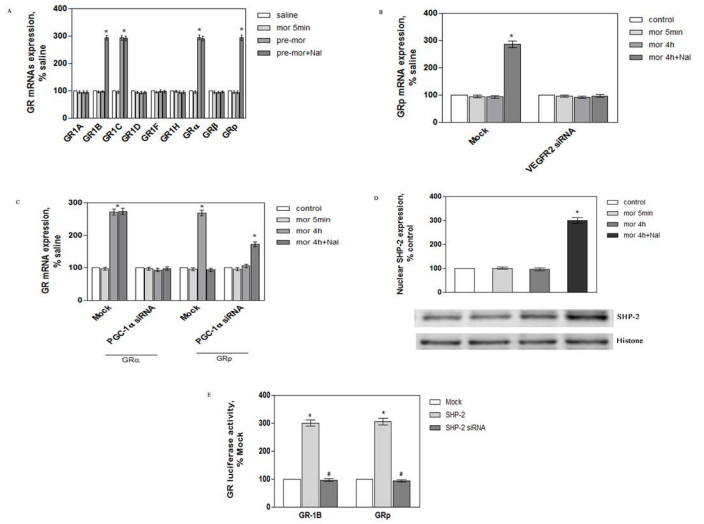

Figure 4. Alternative expression of GR promoters during morphine treatment. A, Mice were undergone chronic morphine treatment and naloxone precipitation, prefrontal cortex was separated. and expressions of GR promoters were detected by real time PCR. B, cortical neurons were grown for 10 days, and co-cultured with vasculature in the presence of VEGFR2 siRNA followed by chronic morphine treatment and subsequent naloxone precipitation, expressions of GR promoters were detected by real time PCR. C, cortical neurons were grown for 10 days, and co-cultured with vasculature in the presence of PGC-1α siRNA followed by chronic morphine treatment and subsequent naloxone precipitation, expressions of GR promoters were detected by real time PCR. D, cortical neurons were grown for 10 days, and co-cultured with vasculature in the presence of morphine for the indicated time, nuclear was separated and SHP-2 expression was determined by Western Blot analysis. E, cortical neurons were grown for 10 days, and co-cultured with vasculature in the presence of SHP-2

or SHP-2 siRNA followed by chronic morphine treatment and subsequent naloxone precipitation, GR-1B and GRp activity was detected by luciferase assay. Data are normalized and calculated as percentage of control, each value represents mean±S.E.M of five independent experiments. *p<0.05 vs control or saline.

Moreover, in neuron-vasculature co-culture, by Western Blot analysis, it was demonstrated that nuclear SHP-2 expression was elevated by naloxone precipitation but not by long-term morphine exposure (Figure 4D). By luciferase assay, it was found that activities of GR-1B and GRp were enhanced by SHP-2 over-expression and decreased by SHP-2 siRNA (Figure 4E).

GR dependent CREB activation during long-term morphine treatment.

It has been reported that CaMKII activation is associated with CREB signaling, and contributes greatly to morphine tolerance and dependence [47-48]. In neuron-vasculature co-culture, we demonstrated that CaMKII expression was evidently elevated following long-term morphine treatment and subsequent naloxone precipitation, intriguingly, the effect of naloxone precipitation was more dependent on GRp than GRα (Figure 5A, B).

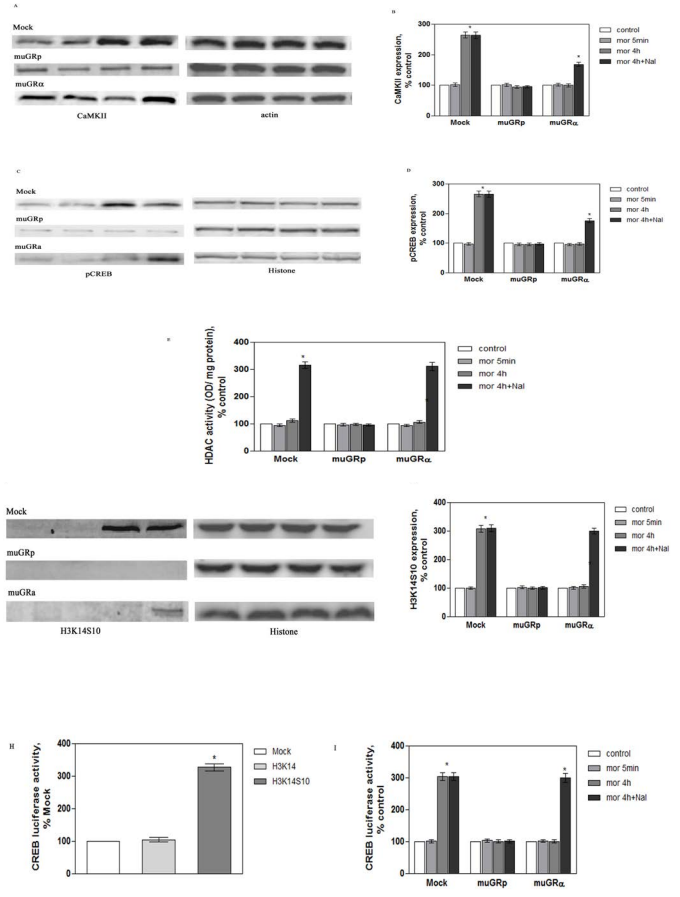

Figure 5. GR dependent CREB activation during long-term morphine treatment. Cortical neurons were grown for 10 days, and co-cultured with vasculature in the presence of mutated GRp/GRα followed by chronic morphine treatment and subsequent naloxone precipitation. A and B, CaMKII activation was measured by Western Blot analysis; C and D, CREB phosphorylation was determined by Western Blot analysis; E, nuclear HDAC activity was determined by photocytometry assay; F and G, histone phosphoacetylation was measured by Western Blot analysis. H, cortical neurons were grown for 10 days, and co-cultured with vasculature in the presence of H3K14 or H3K14S10, CREB activity was detected by luciferase assay. I, cortical neurons were grown for 10 days, and co-cultured with vasculature in the presence of mutated GRp/GRα followed by chronic morphine treatment and subsequent naloxone precipitation, CREB activity was detected by luciferase assay. Data are normalized and calculated as percentage of control, each value represents mean±S.E.M of five independent experiments. *p<0.05 vs control or saline.

Similar alteration happened in CREB phosphorylation (Figure 5C, D). Additionally, HDAC activity and the expression of phosphoacetylated histone (H3K14S10) were enhanced by long-term morphine treatment and subsequent naloxone precipitation, the responses initiated by naloxone precipitation was strongly related with GRp but not GRα (Figure 5E-G). By luciferase assay, it was further revealed that CREB activity was under the control of H3K14S10 (Figure 5H), which was dramatically increased following long-term morphine exposure and subsequent naloxone precipitation, the alteration initiated by naloxone precipitation was also dependent on GRp (Figure 5I).

Vasculature is more sensitive to psychiatric stress

Mice were subjected to cat urine stimulator stress (PSS) for 14 days, then undergone chronic morphine treatment, it was demonstrated that nonmitochondrial sources of oxidant production displayed more increase in the presence of PSS (Figure 6A). As anticipated, similar change pattern was observed in XO/XDH activity (Figure 6B). By real-time PCR and FISH assay, it was illustrated that protein and mRNA expressions of GRα could be up-regulated both by long-term morphine treatment and subsequent naloxone replacement, while GRp was only sensitive to naloxone replacement, significantly, it was GRp but not GRα could be further strengthened in the presence of PSS (Figure 6C-E).

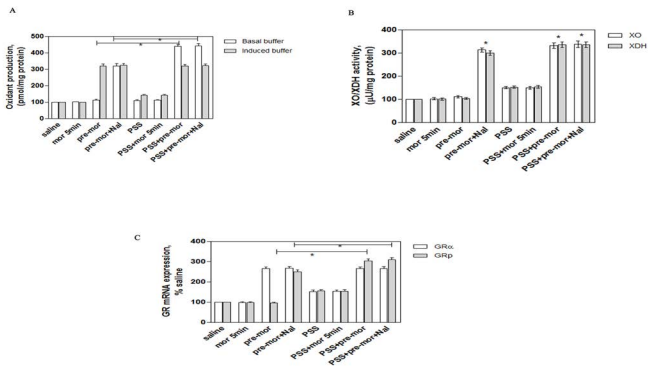

Figure 6. Vasculature is more sensitive to psychiatric stress. Mice were subjected with predator stimulation stress (PSS) for 14 days, then undergone chronic morphine treatment and naloxone precipitation, prefrontal cortex was separated. A, oxidant production in induced or basal buffer were quantified by photocytometry assay, data was converted to pmol/mg protein; B, XO and XOH activity were quantified, data was converted to μU/mg protein; C, mRNA expressions of GRp and GRα were detected by real-time PCR; D and E, FISH assay was performed using GRp and GRα probe and Alexa 488 antibody, each group were analyzed by Leika Q500IW image analysis system, Scale bar=50μm. Data are normalized and calculated as percentage of control, each value represents mean±S.E.M of five independent experiments. *p<0.05 vs saline.

Distinctive effects of GR on morphine dependence and tolerance

Above results promoted to study the functional modulation of morphine dependence and tolerance. Firstly, by counting somatic withdrawal signs including jumps, tremors, wet-dog shakes, rears, and grooming behavior, it was illustrated that, all monitored withdrawal signs were greater in long-term morphine treatment than control animals (jumps: t=10.5, P<0.001; tremors: t=5.25, P<0.001; wet-dog shakes: t=2.75, P<0.05; rears: t=16.2, P<0.001; grooming: t=18.9, P<0.001), the withdrawal effect could be distinctively improved by mutation of GRα or GRp. Additionally, mice in the presence of PSS showed considerably more dependency to morphine, with higher number of withdrawal signs (jumping, rear and grooming) than morphine treatment regimen (Figure7A-D).

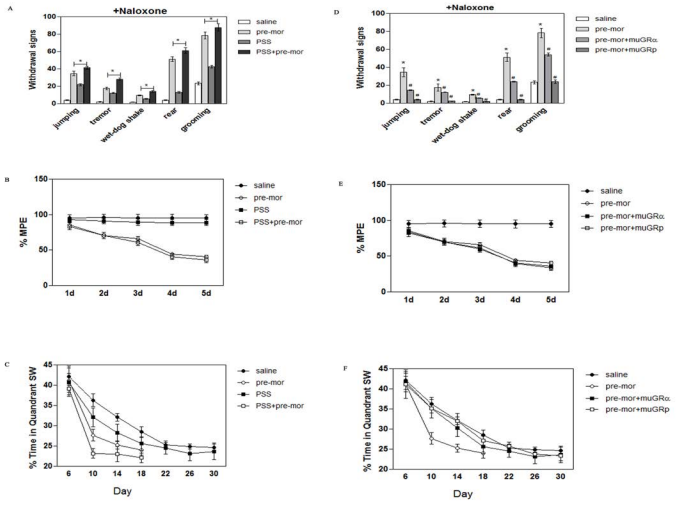

Figure 7. Distinctive effects of GR on morphine dependence and tolerance. Mice were subjected to chronic stress, then undergone chronic morphine treatment and naloxone precipitation (n = 5 for each treatment); or mice were cortical injected adeno-muGRp/GRα followed by chronic morphine treatment and naloxone precipitation (n=5). A and D, mice were placed in the indicated monitor, withdrawal scores including jumping, tremor, wet-dog shake, rear and grooming were measured based on individual signs. B and E, mice were subjected to hot-plate, the cutoff time was set at 10s, antinociceptive response is expressed as the mean with S.E.M. of percentage of the maximum possible effect (%MPE). C and F, mice were placed in the NE quadrant of the water maze without the platform for 60s, amount of time the mice spent in each quadrant searching for the platform was recorded. Probe tests were performed every 4 days afterward until the mice spent an equal amount of time in each quadrant. Data are normalized and calculated, each value represents mean±S.E.M of five independent experiments. *p<0.05 vs saline.

Antinociceptive property of morphine was examined by hot-plate test, a paradigm that primarily assessed supraspinal pain responsiveness [49]. It was demonstrated that onset of morphine tolerance was readily apparent in mice after 2 days of morphine treatment, the degree of tolerance could not be alleviated by mutation of GRα or GRp. Intriguingly, in the presence or absence of PSS, mice displayed similar level of morphine tolerance (Figure7B, E). Finally, mice were placed in the NE quadrant of the water maze without the platform for 60s, the amount of time the mice spent in each quadrant searching for the platform was recorded. It was demonstrated that mice spent less time in SW quadrant following chronic morphine treatment, this performance could be deteriorated in animals subjected to PSS, importantly, the effect was related with GRα or GRp (Figure 7C, F).

Discussion

In the present study, we showed that there was an apparent mitochondrial oxidant production following long-term morphine treatment, while naloxone precipitation equipped a higher capacity in modulation of VEGF-VEGFR2 signaling, thereby, it was postulated that a vascular adapted microenvironment might be established during morphine withdrawal. Moreover, it was shown that VEGFR-2 was related with cAMP overshoot via a close connection with AC5. Since morphine dependence was associated with neuronal opioid receptor-dependent cAMP signal transduction networks, then, the observation was apparently extended to the realization that mitochondrial biogenesis appeared to control MOR desensitization, while VEGF-VEGFR2 signaling might preferentially be manipulated during morphine withdrawal.

It was recognized that chronic opioid use leads to reprogramming of GR-dependent genes. Particularly, there was result showed that the levels of hippocampal GR mRNA are more sensitive to episodes of withdrawal [25-29]. Coincidently, we demonstrated herein that GRα and GRp could be sensitized respectively following long-term morphine exposure and naloxone precipitation. As GR has multiple promoters, studies documented that introns upstream of exons 1B, C, D, F, and H are active promoters [31], among them, the predominantly constitutive nature of promoter 1C is consistently stronger than 1B, D, E, F, J and H [30-32]. In our experiment, it was observed that GR-1C and reflected GRα may be involved in chronic mor-

phine treatment, while GR-1B and reflected GRp were biased initiated following naloxone precipitation. Additionally, we demonstrated that GRp and GRα were functional related with vascular and mitochondrial capacity respectively, and GRp was more responsible for CREB activation than GRα. Then the data indicated that alternative GR promoter usage was proposed to result in different functional consequences and equip an individual capability to adaptive changes in morphine addiction.

As well characterized, stressful experience initiates a neuroendocrine response [53-55], GR activation was found to drive somatodendritic opioid release, resulting in a persistent retrograde suppression of synaptic transmission through presynaptic MOR. In return, stress experience during opioid withdrawal may modify synaptic plasticity and play important roles in drug-associated memory. In our present experiment, predator stimulator stress was established in mice and used as an animal model with persistent GR up-regulation [25-29]. As expected, we found that PSS was in cross-sensitization to morphine, however, with much higher mitochondrial and vascular sensitivity. Finally, we demonstrated that morphine produced expression of somatic withdrawal signs including jumping, tremor, wet-dog shake, rear and grooming, which could be GRp dependently deteriorated when subjected with PSS, similar alteration could be observed in place conditioning performance but not antinociceptive tolerance. Therefore, it was presumed that VEGF-VEGFR2 conditioned vascular remodeling might be predominantly contribute to morphine withdrawal via GRp related transcription machinery, the cellular events might serve as a lynchpin at the intersection of morphine dependence and tolerance.

Conclusion

Altogether, we revealed in prefrontal cortex, that there was apparent mitochondrial and vascular oxidant production following long-term morphine treatment and subsequent naloxone precipitation. Comparably, naloxone precipitation equipped a capacity in modulation of VEGF-VEGFR2 signaling and a close connection of VEGFR2 and AC5. Moreover, there was alternative GR promoter usage that was related with vascular and mitochondrial sensitivity, GR-1C and reflected GRα were involved in chronic morphine treatment, while GR-1B and reflected GRp were biased initiated following naloxone precipitation, the distinctive alteration equipped an individual capability to mediate CREB expression and phosphorylation. Of most interest, by using mice subjected to predator stimulator stress (PSS), it was visualized that PSS was in cross-sensitization to morphine, however, with much higher capacity in oxidant production and CREB activation. Intriguingly, mice with PSS exhibited deteriorated behaviors in terms of morphine withdrawal and place conditioning, but not antinociceptive tolerance, the responses were more related with GRp than GRα. Therefore, our results unveiled a pivotal role of mitochondrial and vascular environment in the maintaining and potentiation of neuro-adaptive morphine activities, in which increasing vulnerability of GRp to vascular remodeling was thought to be critical for morphine withdrawal.

Acknowledgements

The study was supported by National Nature Sciences of China (81471370).

References

1. Nestler EJ. Molecular neurobiology of addiction. Am J Addict. 2001, 10: 201-217.

2. Nestler EJ. Historical review: Molecular and cellular mechanisms of opiate and cocaine addiction. Trends Pharmacol. Sci. 2004, 25(4): 210-218.

3. Matthes HW, Maldonado R, Simonin F, Valverde O, Slowe S et al. Loss of morphine-induced analgesia, reward effect and withdrawal symptoms in mice lacking the mu-opioid-receptor gene. Nature. 1996, 383(6603): 819-823.

4. Mello NK, Negus SS. Preclinical evaluation of pharmacotherapies for treatment of cocaine and opioid abuse using drug self-administration procedures. Neuropsychopharmacology 1996, 14(6): 375-424.

5. Sora I, Funada M, Uhl GR. The mu-opioid receptor is necessary for [D-Pen2,D-Pen5] enkephalin-induced analgesia. Eur J Pharmacol. 1997, 234(3): R1-2.

6. Sharma SK, Nirenberg M, Klee WA. Morphine receptors as regulators of adenylate cyclase activity. Proc Natl Acad Sci. USA. 1975, 72(2): 590-594.

7. Sharma SK, Klee WA, Nirenberg M. Opiate-dependent modulation of adenylate cyclase. Proc. Natl. Acad. Sci. U. S. A. 1977, 74(8): 3365-3369.

8. Chao J, Nestler EJ. Molecular neurobiology of drug addiction. Annu. Rev. Med. 2004, 55: 113-132.

9. Christie MJ. Cellular neuroadaptations to chronic opioids: tolerance, withdrawal and addiction. Br. J Pharmacol. 2008, 154: 384-396.

10. Koob GF, Bloom FE. Cellular and molecular mechanisms of drug dependence. Science 1988, 242: 715-723.

11. McClung CA, Nestler EJ, Zachariou V. Regulation of gene

expression by chronic morphine and morphine withdrawal in the locus ceruleus and ventral tegmental area. J. Neurosci. 2005, 25: 6005-6015.

12. Watts VJ. Molecular mechanisms for heterologous sensitization of adenylate cyclase. J Pharmacol. Exp. Ther. 2002, 302: 1-7.

13. Liu L, Coller JK, Watkins LR, Somogyi AA, Hutchinson MR. Naloxone-precipitated morphine withdrawal behavior and brain IL-1β expression: comparison of different mouse strains. Brain Behav. Immun. 2011, 25: 1223-1232.

14. Schwarz JM, Hutchinson MR, Bilbo SD. Early-life experience decreases drug-induced reinstatement of morphine CPP in adulthood via microglial-specific epigenetic programming of anti-inflammatory IL-10 expression. J Neurosci. 2011, 31: 17835-17847.

15. Johnston IN, Milligan ED, Wieseler-Frank J, Frank MG et al.A role for proinflammatory cytokines and fractalkine in analgesia, tolerance, and subsequent pain facilitation induced by chronic intrathecal morphine. J Neurosci. 2004, 24: 7353-7365.

16. Johnston IN, Westbrook RF. Inhibition of morphine analgesia by LPS: role of opioid and NMDA receptors and spinal glia. Behav. Brain Res. 2005, 156: 75-83.

17. Raghavendra V, Rutkowski MD, DeLeo JA. The role of spinal neuroimmune activation in morphine tolerance/hyperalgesia in neuropathic and sham-operated rats. J. Neurosci. 2002, 22: 9980-9989.

18. Basuroy S, Bhattacharya S, Leffler CW, Parfenova H. Nox4 NADPH oxidase mediates oxidative stress and apoptosis caused by TNF-alpha in cerebral vascular endothelial cells. Am. J. Physiol. Cell Physiol. 2009, 296: C422–C432.

19. Dopp JM, Philippi NR, Marcus NJ, Olson EB, Bird CE et al. Xanthine oxidase inhibition attenuates endothelial dysfunction caused by chronic intermittent hypoxia in rats. Respiration. 2011, 82: 458–467.

20. Jackson MJ. Control of reactive oxygen species production in contracting skeletal muscle. Antioxidants Redox. Signal. 2011, 15: 2477–2486.

21. Klitzman B, Damon DN, Gorczynski RJ, Duling BR. Augmented tissue oxygen supply during striated muscle contraction in the hamster. Relative contributions of capillary recruitment, functional dilation, and reduced tissue PO2. Circulation Res. 1982, 51: 711–721.

22. Zhang C, Xu X, Potter BJ, Wang W, Kuo L et al. TNF-alpha contributes to endothelial dysfunction in ischemia/reperfusion injury. Arteriosclerosis, Thrombosis Vascular Biol. 2006, 26: 475–480.

23. Zhao H, Wu GC, Cao X. EGFR dependent subcellular communication was responsible for morphine mediated AC superactivation. Cell Signal. 2013, 25: 417-428.

24. Zhao H, Huang HW, Wu JG, Huang PY. Specialization of mitochondrial and vascular oxidant modulated VEGFR in the denervated skeletal muscle. Cell Signal. 2013, 25: 2106-2114.

25. Slezak M, Korostynski M, Gieryk A, Golda S, Dzbek J et al. Astrocytes are a neural target of morphine action via glucocorticoid receptor-dependent signaling. Glia 2013, 61: 623-635.

26. Dong Z, Han H, Cao J, Xu L. Opioid withdrawal for 4 days prevents synaptic depression induced by low dose of morphine or naloxone in rat hippocampal CA1 area in vivo. Hippocampus. 2010, 20: 335-343.

27. Yang Y, Zheng X, Wang Y, Cao J, Dong Z et al. Stress enables synaptic depression in CA1 synapses by acute and chronic morphine: possible mechanisms for corticosterone on opiate addiction. J. Neurosci. 2004, 24: 2412-2420.

28. McNally GP, Akil H. Selective down-regulation of hippocampal glucocorticoid receptors during opiate withdrawal. Brain Res Mol Brain Res. 2003, 118(1-2): 152-155.

29. Wamsteeker Cusulin JI, Füzesi T, Inoue W, Bains JS. Glucocorticoid feedback uncovers retrograde opioid signaling at hypothalamic synapses. Nat Neurosci. 2013, 16: 596-604.

30. Trollope AF, Gutierrez-Mecinas M, Mifsud KR, Cilloins A, Sounder EA et al. Stress, epigenetic control of gene expression and memory formation. Exp Neurol 2012, 233: 3-11.

31. Turner JD, Alt SR, Cao L, Vernocchi S, Trifonova S et al. Transcriptional control of the glucocorticoid receptor, CpG island, epigenetics and more. Biochem Pharmacol. 2010, 80: 1860-1868.

32. Cao L, Leija SC, Kumsta R, Wust S, Meyer J, Turner JD, Muller CP. Transcriptional control of the human glucocorticoid receptor: identification and analysis of alternative promoter regions. Hum Henet 2011, 129: 533-543.

33. Oh DH, Kim BW, Choi M, Lee G, Choi JS et al. Changes in vascular endothelial growth factor (VEGF) induced by the Morris water maze task. Mol Cells 2012, 33(8): 295-300.

34. Berke JD, Hyman SE. Addiction, dopamine, and the molecular mechanisms of memory. Neuron. 2000, 25: 515-532.

35. Leick L, Wojtaszewski JF, Johansen ST, Kiilerich K, Comes G et al. PGC-1alpha is not mandatory for exercise- and training-induced adaptive gene responses in mouse skeletal muscle. Am. J. Physiol. Endocrinol. Metab. 2008, 294: E463–E474.

36. Leick L, Hellsten Y, Fentz J, Lyngby SS, Wojtaszewski JF et al. PGC-1alpha mediates exercise-induced skeletal muscle VEGF expression in mice. Am. J. Physiol. Endocrinol. Metab. 2009, 297: E92–E103.

37. Leick L, Lyngby SS, Wojtasewski JF, Pilegaard H. PGC-1alpha is required for training-induced prevention of age-associated decline in mitochondrial enzymes in mouse skeletal muscle. Exp. Gerontol. 2010, 45: 336–342.

38. Carlezon WA Jr, Duman RS, Nestler EJ. The many faces of CREB. Trends Neurosci. 2005, 28: 436-445.

39. Nestler EJ, Carlezon WA Jr. The mesolimbic dopamine reward circuit in depression. Biol. Psychiatry 2006, 59: 1151-1159.

40. Turgeon SM, Pollack AE, Fink JS. Enhanced CREB phosphorylation and changes in c-Fos and FRA expression in striatum accompany amphetamine sensitization. Brain Res. 1997, 749: 120-126.

41. Lane-Ladd SB, Pineda J, Boundy VA, Pfeuffer T, Krupinski J et al. CREB (cAMP response element-binding protein) in the locus coeruleus: biochemical, physiological, and behavioral evidence for a role in opiate dependence. J. Neurosci. 1997, 17: 7890-7901.

42. Maldonado R, Blendy JA, Tzavara E, Gass P, Roques BP et al. Reduction of morphine abstinence in mice with a mutation in the gene encoding CREB. Science 1996, 273: 657-659.

43. Montminy M. Transcriptional activation. Something new to hang your HAT on. Nature 1997, 387: 654-655.

44. Shaywitz AJ, Greenberg ME. CREB: a stimulus-induced transcription factor activated by a diverse array of extracellular signals. Annu. Rev. Biochem. 1999, 68: 821-861.

45. Silva AJ, Kogan JH, Frankland PW, Kida S. CREB and memory. Annu. Rev. Neurosci. 1998, 21: 27-48.

46. Widnell KL, Russell DS, Nestler EJ. Regulation of expression of cAMP response element-binding protein in the locus coeruleus in vivo and in a locus coeruleus-like cell line in vitro. Proc. Natl. Acad. Sci. U S A. 1994, 91: 10947-10951.

47. Wang ZJ, Wang LX. Phosphorylation: a molecular switch in opioid tolerance. Life Sci 2006, 79: 1681-1691.

48. Illing S, Mann A, Schulz S. Heterologous regulation of agonist-independent ?-opioid receptor phosphorylation by protein kinase C. Br. J. Pharmacol. 2014, 171: 1330-1340.

49. Bohn LM, Lefkowitz RJ, Gainetdinov RR, Peppel K, Caron MG, Lin FT. Enhanced morphine analgesia in mice lacking beta-arrestin 2. Science 1999, 286: 2495-2498.

50. Terwilliger RZ, Beitner-Johnson D, Sevarino KA, Crain SM, Nestler EJ. A general role for adaptations in G-proteins and the cyclic AMP system in mediating the chronic actions of morphine and cocaine on neuronal function. Brain Res. 1991, 548: 100-110.

51. Han MH, Bolanos CA, Green TA, Olson VG, Neve RL, Liu RJ et al. Role of cAMP response element-binding protein in the rat locus ceruleus: regulation of neuronal activity and opiate withdrawal behaviors. J. Neurosci. 2006, 26: 4624-4629.

52. Shaw-Lutchman TZ, Barrot M, Wallace T, Gilden L, Zachariou V et al. Regional and cellular mapping of cAMP response element-mediated transcription during naltrexone-precipitated morphine withdrawal. J. Neurosci. 2002, 22: 3663-3672.

53. Myers B, McKlveen JM, Herman JP. Glucocorticoid actions on synapses circuits and behavior: implications for the energetic of stress. Front Neuroendocrinol 2014, 35: 180-196.

54. Romeo RD, McEwen BS. Stress and the adolescent brain. Ann N Y Acad Sci 2006, 1094: 202-214.

55. Smith SM, Vale WW. The role of the hypothalamic-pituitary-adrenal axis in the neuroendocrine responses to stress. Dialogues Clin. Neurosci. 2006, 6: 383-395.